DINCON 2019 ID: 1986
XIV CONFERÊNCIA BRASILEIRA DE DINÂMICA, CONTROLE E APLICAÇÕES
25 de novembro a 27 de novembro de 2019 – São Carlos/SP

Finite element simulation of microswimmers

Stevens Paz Sánchez[1]
Instituto de Ciências Matemáticas e de Computação
USP, São Carlos, SP
Gustavo C. Buscaglia[2]
Instituto de Ciências Matemáticas e de Computação
USP, São Carlos, SP

Abstract. Forces and velocities acting tangentially at the surface of a microparticle activate the swimming capacity of the body immersed in an ambient fluid dominated by viscous forces. The configurations, or states, of this microswimmer become in unknowns of the corresponding fluid-solid interaction problem, coupled to the equations describing the fluid's dynamics. We present a finite element method capable of dealing with this kind of interfacial interactions, detailing the good function spaces and the variational formulation. We apply this formulation to numerically compute the swimming of two squirmers living in low-Reynolds regimes.

Keywords. Microswimmer, Slip Velocity, Finite Element Method, Generalized Coordinates.

1 Introduction

The most used strategy to simulate squirmers, which are models of microparticles that swim via small shape oscillations [3], are those based on boundary element methods [6], having the advantage of requiring little need of remeshing along the squirmers evolution, and dealing, principally, with spherical-shaped swimmers, but limited to the problem's linearity.

On the other hand, formulations based on finite element methods (FEM) can easily deal with with non-zero Reynolds numbers regimes, non-Newtonian rheology and non-linear model configurations, turning them into a very attractive option for many applications like self-learning swimming of microrobots, in which the knowledge of accurate fluid velocity and pressure fields, as well as interaction forces, is crucial to feed machine learning algorithms [7, 8].

[1]espeisan@usp.br
[2]gustavo.buscaglia@icmc.usp.br

In this work we present a FEM formulation to deal with fluid-solid interaction (FSI) problems dealing, specifically, with the successful simulation of squirmers of any shape, like microorganism or articulated microstructures.

2 Kinematics of squirmers

In this letter we focus on swimmers modeled as rigid bodies, so all their possible configurations are images $\mathcal{B}$ of a reference domain $\mathcal{B}^* \subset \mathbb{R}^d$, $d = 2, 3$, by the action of translations and rotations, which are the generalized coordinates of the mechanical system. Defining a point $\mathbf{X}_c$ as center of rotation, at all times t there exists a point $\mathbf{x}_c(t)$ and a rotation matrix $\mathbf{Q}(t)$ such that the position $\mathbf{x}(\mathbf{X}, t)$ of the material point $\mathbf{X}$ is given by $\mathbf{x}(\mathbf{X}, t) = \mathbf{x}_c(t) + \mathbf{Q}(t)(\mathbf{X} - \mathbf{X}_c)$.

The manifold of possible configurations of the squirmer is $Q = \mathbb{R}^d \times \mathsf{SO}(d)$, where $\mathsf{SO}(d) = \left\{\mathbf{Q} \in \mathbb{R}^{d\times d} : \mathbf{Q}^{-1} = \mathbf{Q}^T, \det[\mathbf{Q}] = 1\right\}$, and the body's Eulerian velocity $\mathbf{u}_\mathcal{B}$ is given by $\mathbf{u}_\mathcal{B}(\mathbf{x}, t) = \mathbf{v}_c(t) + \boldsymbol{\omega}(t) \times (\mathbf{x} - \mathbf{x}_c(t)) = \mathbf{H}(\mathbf{q}(t), \mathbf{x})\,\mathbf{s}(t)$, where $\mathbf{v}_c(t) = \dot{\mathbf{x}}_c(t)$ is the translational velocity and $\boldsymbol{\omega}(t)$ is the pseudovector of angular velocities in the spatial frame, which relates to $\mathbf{Q}(t)$ and $\dot{\mathbf{Q}}(t)$ by $\dot{\mathbf{Q}}\mathbf{Q}^T = \mathrm{sk}[\boldsymbol{\omega}]$ where the isomorphism sk[·] between vectors and skew-symmetric matrices is the classic skew-symmetric operator. The velocity array is $\mathbf{s} = (\mathbf{v}_c, \boldsymbol{\omega})^T \in \mathbb{R}^{n_c}$, $n_c = d + \frac{d(d-1)}{2}$.

The Navier-Stokes equations describe the dynamics of the ambient fluid, namely,

$$\rho\frac{D\mathbf{u}}{Dt} - \nabla\cdot\boldsymbol{\sigma} = \mathbf{0} \text{ and } \nabla\cdot\mathbf{u} = 0 \text{ in } \Omega_f(t), t \in (0, T),$$

where ρ is the density, $\mathbf{u}$ the Eulerian velocity field, D/Dt the material derivative and $\boldsymbol{\sigma}$ the Cauchy stress tensor. Although other rheological models can be considered, for simplicity we will assume a quasi-Newtonian fluid, i.e., $\boldsymbol{\sigma} = -p\,\mathbf{I}_d + 2\mu\nabla^S\mathbf{u}$, where p is the pressure, μ is the (possibly shear-rate dependent) viscosity and $\nabla^S\mathbf{u} = \frac{1}{2}\left(\nabla\mathbf{u} + \nabla\mathbf{u}^T\right)$.

3 The FSI model and FEM discretization

Here we present a basic description of the fluid-solid model configuration aiming the presentation of a variational formulation for our interaction problem, a detailed explanation of this formulation can be found in [5]. The immersed body $\mathcal{B}$ contributes to the dynamics of the ambient fluid through *boundary conditions* at $\partial\mathcal{B}$ as well as *kinematical conditions*, in which some slip velocity $\mathbf{u}_s$ is defined as $\mathbf{u}(\mathbf{x}, t) = \mathbf{u}_\mathcal{B}(\mathbf{x}, t) + \mathbf{u}_s(\mathbf{x}, t)$, $\forall\mathbf{x} \in \partial\mathcal{B}(t)$, $\forall t$, and *tangential force equilibrium* by means of a force $\mathbf{f}_s$ exerted by the squirmer on the adjacent fluid, satisfying $\mathbf{P}_{\boldsymbol{\tau}}\,\boldsymbol{\sigma}(\mathbf{x}, t)\,\mathbf{n} = \mathbf{f}_s(\mathbf{x}, t)$, $\mathbf{x} \in \partial\mathcal{B}(t)$, $t \geq 0$, where $\mathbf{P}_{\boldsymbol{\tau}} = \mathbf{I}_d - \mathbf{n}\,\mathbf{n}^T$ is the projection matrix onto the tangent plane to $\partial\mathcal{B}(t)$ at $\mathbf{x}$, with normal unit vector $\mathbf{n}$ pointing into the body.

The mathematical problem reads as follows: Given $\mathbf{q}(t = 0)$ and $\mathbf{u}(\mathbf{x}, t = 0)$ (this latter datum is only needed if $\rho > 0$), determine $\mathbf{q}(t) = (\mathbf{x}_c(t), \mathbf{Q}(t))$, $\mathbf{s}(t) = (\mathbf{v}_c(t), \boldsymbol{\omega}(t))$,

$\mathbf{u}(\mathbf{x},t)$ and $p(\mathbf{x},t)$ for $0<t\leq T$ and $\mathbf{x}\in\Omega_f(t)$ satisfying

$$\frac{d\mathbf{x}_c}{dt} = \mathbf{v}_c, \tag{1}$$

$$\frac{d\mathbf{Q}}{dt} = \mathrm{sk}\left[\boldsymbol{\omega}\right]\mathbf{Q}, \tag{2}$$

$$\mathbf{u}\left(\mathbf{x},t\right)-\mathbf{H}\left(\mathbf{q}(t),\mathbf{x}\right)\mathbf{s}(t) = \mathbf{u}_s\left(\mathbf{x},t\right), \qquad \text{on } \partial\mathcal{B}\left(t\right), \tag{3}$$

$$\rho\frac{D\mathbf{u}}{Dt}-2\nabla\cdot\left(\mu\,\nabla^S\mathbf{u}\right)+\nabla p = \mathbf{0}, \qquad \text{in } \Omega_f(t), \tag{4}$$

$$\nabla\cdot\mathbf{u} = 0, \qquad \text{in } \Omega_f(t), \tag{5}$$

$$\int_{\partial\mathcal{B}(t)}\boldsymbol{\sigma}\,\mathbf{n}\;dS = \mathbf{0}, \tag{6}$$

$$\int_{\partial\mathcal{B}(t)}\left(\mathbf{x}-\mathbf{x}_c\right)\times\boldsymbol{\sigma}\,\mathbf{n}\;dS = \mathbf{0}. \tag{7}$$

The variational problem is formulated on the function space [1]

$$W\left(\mathbf{q}\right)=\left\{\mathbf{w}\in H^1\left(\Omega_f(\mathbf{q})\right)^d\,:\mathbf{w}=\mathbf{0}\text{ on }\partial\Omega,\ \mathbf{w}=\mathbf{H}(\mathbf{q})\mathbf{d}\text{ on }\partial\mathcal{B},\ \mathbf{d}\in\mathbb{R}^{n_c}\right\},$$

decomposed as $W\left(\mathbf{q}\right)=W_0\left(\mathbf{q}\right)\oplus V\left(\mathbf{q}\right)$, where $V(\mathbf{q})$ is the finite-dimensional space (of dimension n_c) of extensions of rigid-body motions, i.e., $V(\mathbf{q})=\{\mathbf{w}\in H^1\left(\Omega_f\left(\mathbf{q}\right)\right)^d\,:\,\mathbf{w}=\mathcal{E}\,\mathbf{H}(\mathbf{q})\,\mathbf{d},\ \mathbf{d}\in\mathbb{R}^{n_c}\}$ and $W_0=H^1\left(\Omega_f\left(\mathbf{q}\right)\right)^d$. Here, $\mathcal{E}$ is an extension linear operator that, given a (regular enough) function f defined on $\partial\mathcal{B}$, assigns to it $\mathcal{E}f\in H^1(\Omega_f)$ that coincides with f on $\partial\mathcal{B}$ and is zero on $\partial\Omega$. The action of this operator on vector or matrix fields defined on $\partial\mathcal{B}$ is defined by applying $\mathcal{E}$ componentwise. Also, $\mathbf{H}\left(\mathbf{q}\right)\mathbf{d}$ is the vector field defined on $\partial\mathcal{B}$ by $\left[\mathbf{H}\left(\mathbf{q}\right)\mathbf{d}\right]\left(\mathbf{x}\right)=\mathbf{H}\left(\mathbf{q},\mathbf{x}\right)\mathbf{d}$. We denote $\widetilde{\mathbf{H}}(\mathbf{q})=\mathcal{E}\mathbf{H}(\mathbf{q})$.

The weak formulation of (3)-(7) reads as follows: *Find* $(\mathbf{s}(t),\mathbf{u},p)$*, where* $\mathbf{u}$ *must belong to* $\mathcal{E}\mathbf{u}_s+\widetilde{\mathbf{H}}(\mathbf{q}(t))\,\mathbf{s}(t)+W_0(\mathbf{q}(t))$ *and* p *must belong to* $L^2_0(\Omega_f(t))$*, such that*

$$\int_{\Omega_f(t)}\rho\,\frac{D\mathbf{u}}{Dt}\left(\mathbf{x},t\right)\cdot\mathbf{w}\left(\mathbf{x}\right)\,d\mathbf{x}+\int_{\Omega_f(t)}\boldsymbol{\sigma}\left(\mathbf{x},t\right):\nabla^S\mathbf{w}\left(\mathbf{x}\right)\,d\mathbf{x} = 0,$$

$$\int_{\Omega_f(t)}z\left(\mathbf{x}\right)\nabla\cdot\mathbf{u}\left(\mathbf{x},t\right)\,d\mathbf{x} = 0,$$

for all $(\mathbf{w},z)\in W\left(\mathbf{q}(t)\right)\times L^2_0(\Omega_f(t))$.

In a triangulation Ω_{fh} of the fluid domain, being $h>0$ a characteristic size, the fluid velocity and pressure approximations take the form $\mathbf{u}_h\left(\mathbf{x},t\right)=\sum_{j\in\eta^U}\mathcal{N}^j\left(\mathbf{x},t\right)\mathbf{u}^j\left(t\right)$ and $p_h\left(\mathbf{x},t\right)=\sum_{k\in\eta^P}\mathcal{M}^k\left(\mathbf{x},t\right)p^k\left(t\right)$, for $\mathbf{x}\in\overline{\Omega}_{fh}\left(t\right)=\bigcup_e\Omega^e\left(t\right)$, in finite dimensional subspaces $U_h\left(t\right)\subset H^1\left(\Omega_f\left(t\right)\right)^d$ and $M_h\left(t\right)\subset L^2_0(\Omega_f(t))$. The shape functions $\mathcal{N}^j\left(\cdot,t\right)$, $\mathcal{M}^k\left(\cdot,t\right)$ satisfy the nodal value property, namely, $\mathcal{N}^j\left(\mathbf{x}^i(t),t\right)=\delta_{ij}$ (Kronecker delta), where $\mathbf{x}^i(t)$ is the position of node i in the mesh, for i belonging to the velocity global index set η^U. In particular, $\mathbf{u}_h\left(\mathbf{x}^i,t\right)=\mathbf{u}^i\left(t\right)$, for all $i\in\eta^U$. Similarly, $\mathcal{M}^k\left(\mathbf{x}^l(t),t\right)=\delta_{kl}$, so that $p_h\left(\mathbf{x}^l(t),t\right)=p^l(t)$ for pressure nodes $\mathbf{x}^l$ indexed by the set η^P. The interpolation space for the velocity is

$$U_h\left(\mathbf{q}\right)=\left\{\mathbf{w}\in H^1\left(\Omega_{fh}\left(\mathbf{q}\right)\right)^d\,:\,\mathbf{w}\big|_{\Omega^e}\in P_m\left(\Omega^e\right)^d,\ \text{for all } e,\ \mathbf{w}\big|_{\partial\Omega}=\mathbf{0}\right\},$$

and for the pressure

$$M_h(\mathbf{q}) = \left\{ q \in L_0^2(\Omega_{fh}(\mathbf{q})) \,:\, q\big|_{\Omega^e} \in P_m(\Omega^e),\ \text{for all } e \right\},$$

where $P_m(\Omega^e)$ is the space of polynomials in Ω^e of degree less than or equal to m. Here we consider a GLS stabilized P_1/P_1 element.

Introducing the spaces

$$W_h(\mathbf{q}) = \left\{ \mathbf{w}_h \in U_h(\mathbf{q}) \,:\, \mathbf{w}_h = \mathbf{0} \text{ on } \partial\Omega,\ \mathbf{w}_h = \mathbf{H}(\mathbf{q})\mathbf{d} \text{ on } \partial\mathcal{B}_h,\ \mathbf{d} \in \mathbb{R}^{n_c} \right\}$$
$$W_{0h}(\mathbf{q}) = \left\{ \mathbf{w}_h \in U_h(\mathbf{q}) \,:\, \mathbf{w}_h = \mathbf{0} \text{ on } \partial\Omega,\ \mathbf{w}_h = \mathbf{0} \text{ on } \partial\mathcal{B}_h \right\},$$

the semidiscrete formulation then reads: *Determine functions* $\mathbf{q}_h(t) = (\mathbf{x}_{ch}(t), \mathbf{Q}_h(t)) : [0,T] \to Q$, $\mathbf{s}_h(t) = (\mathbf{v}_{ch}(t), \boldsymbol{\omega}_h(t)) : [0,T] \to \mathbb{R}^{n_c}$, $\mathbf{u}_h(\cdot,t) \in W_h(\mathbf{q}_h(t))$ *and* $p_h(\cdot,t) \in M_h(\mathbf{q}_h(t))$ *such that*

$$\mathbf{u}_h(\cdot,t) - \widetilde{\mathbf{H}}(\cdot,t)\mathbf{s}_h(t) - \mathcal{E}\mathbf{u}_{sh}(\cdot,t) \in W_{0h}(\mathbf{q}_h(t)) \tag{8}$$

and

$$\frac{d\mathbf{x}_{ch}}{dt} - \mathbf{v}_{ch} = \mathbf{0}, \tag{9}$$
$$\frac{d\mathbf{Q}_h}{dt} - \mathrm{sk}[\boldsymbol{\omega}_h]\,\mathbf{Q}_h = \mathbf{0}, \tag{10}$$
$$\int_{\Omega_{fh}} \rho \frac{D\mathbf{u}_h}{Dt} \cdot \mathbf{w}_h \, d\mathbf{x} + \int_{\Omega_{fh}} 2\mu(\nabla^S \mathbf{u}_h)\nabla^S \mathbf{u}_h : \nabla^s \mathbf{w}_h \, d\mathbf{x} - \int_{\Omega fh} p_h \nabla \cdot \mathbf{w}_h \, d\mathbf{x} = 0, \tag{11}$$
$$\int_{\Omega_{fh}} z_h \nabla \cdot \mathbf{u}_h \, d\mathbf{x} = 0, \tag{12}$$

for all $\mathbf{w}_h \in W_h(\mathbf{q}_h(t))$, *for all* $z_h \in M_h(\mathbf{q}_h(t))$, *for all* t.

4 Squirmer simulations

4.1 A toroidal swimmer

The rotation of a circle of radius $r_c > 0$, around an axis of symmetry, generates a torus $\mathcal{B}$ when the distance α from its center to this axis satisfies $\alpha > r_c$. Defining the parameter $\delta = \frac{\alpha - r_c}{r_c}$, we simulate the flux surrounding a slippery torus when varying δ from 5×10^{-3} to 2×10^2 using $P1/P1$ GLS stabilized finite element space.

Initially, a tangential velocity $\mathbf{u}_s = \boldsymbol{\tau}$, with constant magnitude and living in the radial-axial plane, is imposed at the surface of the swimmer, as shown in Figure 1. The swimmer moves in the positive direction of the axis of symmetry due to fluid that is injected from the rear of the torus and passing by the reduced interior region. The speed v_c of the swimmer decreases when δ increases because fluid has more liberty to flow in the interior region, as shown in Figure 2 by the blue curve. The Figure 1 presents the fluid velocity

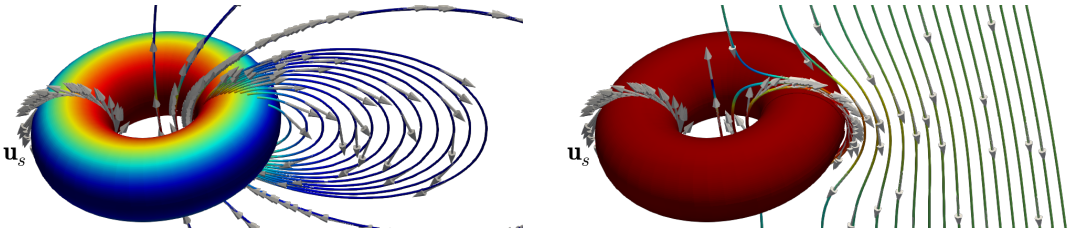

Figure 1: Fluid velocity streamlines around the swimmer, generated by imposing the slip velocity $\mathbf{u}_s$; the direction of the velocity field is indicated by normalized vectors in the laboratory frame (left) and in a frame moving with the torus (right). The colors going from red to blue indicate maximum to minimum velocity magnitude. Both cases correspond to $\delta = 1$.

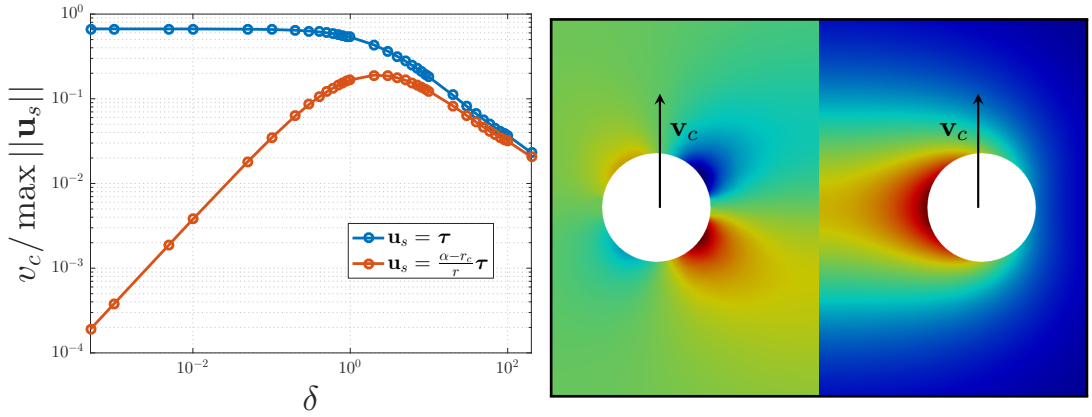

Figure 2: Left: Translational speed of the toroidal swimmer as a function of δ for the considered slip velocities. Right: Fluid pressure (left) and velocity magnitude (right) when imposing $\mathbf{u}_s = \frac{\alpha - r_c}{r}\boldsymbol{\tau}$ for $\varepsilon = 2$, plotted in a cross-section of the swimmer. The black arrows indicate the direction of movement. The colors going from red to blue indicate maximum to minimum velocity magnitude and pressure.

streamlines around the swimmer both in laboratory and moving with the torus frame of reference for $\delta = 1$.

A spherical squirmer driven by a slip velocity with zero mean does not swim [2]. What would happen to a toroidal swimmer? A second case amounts to impose the slip velocity $\mathbf{u}_s = \frac{\alpha - r_c}{r}\boldsymbol{\tau}$ whose mean value on the torus' surface is null, where r is the radial coordinate of a point in $\partial\mathcal{B}$, which means that the contribution of the slip velocity will be concentrated in the surface region nearest to the axis of symmetry. In this configuration, the body $\mathcal{B}$ also gains positive translational velocity as depicted in Figure 2: the speed is low for small values of δ and increases up to a maximum speed, when $\delta = 2$, and then decays similarly to the case of slip velocity with constant magnitude. The fluid velocity magnitude and pressure is presented in Figure 2 for $\delta = 2$.

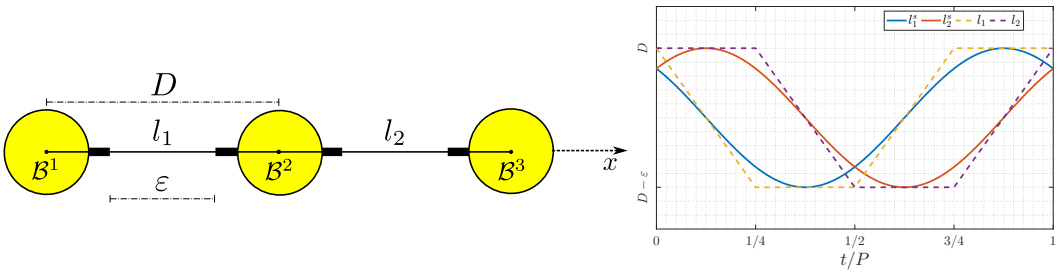

Figure 3: Left: 3-linked spheres swimmer. Right: Links length as functions of dimensionless time t/P.

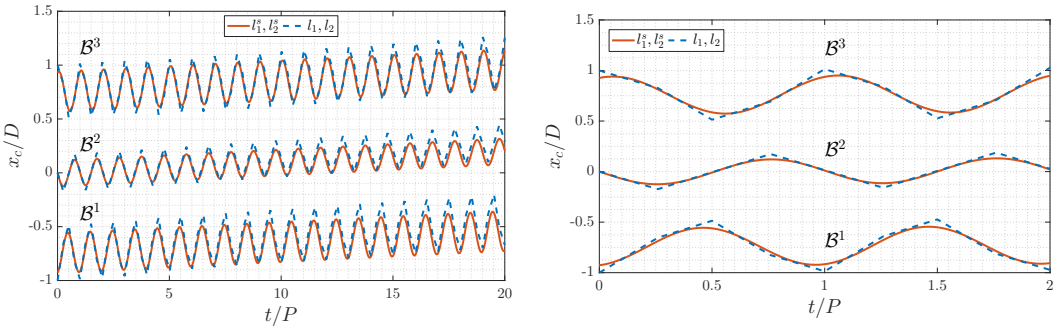

Figure 4: Left: Position of the center of mass for each sphere in the swimmer, scaled by the maximum length D, for each swimming strategy. Right: Detailed view of the center of mass displacement at the first two periods.

4.2 3-linked spheres

The 3-linked spheres swimmer model (Figure 3) was introduced by [4] considering the bodies' arms having negligible thickness and performing a non-reciprocal sequence of contractions and expansions given by the piecewise linear functions (of time) l_1 and l_2 shown in Figure 3 (dashed curve). This periodic swimming strategy, with period P, induces a non-null net displacement of the swimmer in the axial direction. The maximum and minimum length of the links in a period are denoted by D and $D-\varepsilon$, respectively, with $0 < \varepsilon < 2r$, being $r > 0$ the radii of the spheres. We simulate this classic swimming strategy as well as a smoothed version of it, resulting from considering the sinusoidal functions l_1^s and l_1^s, also shown in Figure 3 (continuous line).

The center of mass x_c of each sphere oscillates according to the dynamics of the links, inducing a displacement of the whole swimmer. Figure 4 shows the path followed by each sphere evidencing that, for each swimming strategy, namely, the linear piecewise and the sinusoidal, the swimmer advances in the axial direction. The Figure 5 depicts the fluid velocity magnitude and the pressure when using the second swimming strategy.

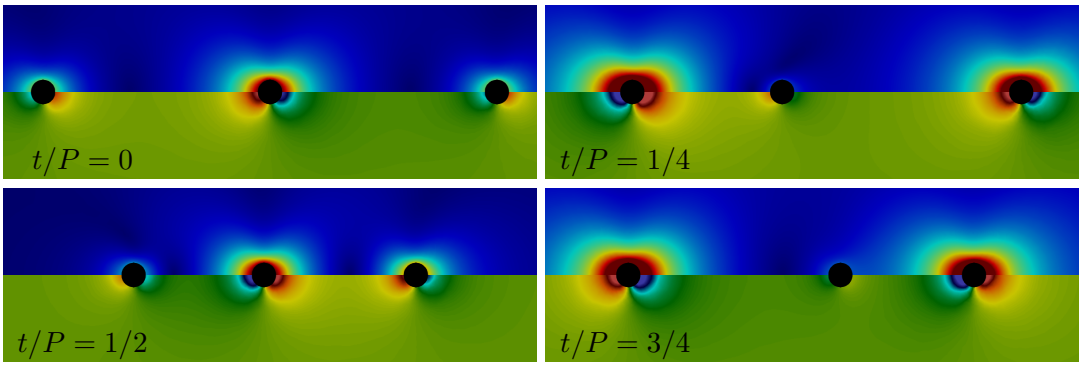

Figure 5: Fluid velocity magnitude (upper region on each graphic) and pressure (lower region on each graphic) at different times. The spheres in the swimmer are colored in black. The colors going from red to blue indicate maximum to minimum velocity magnitude and pressure.

References

[1] R. Glowinski, T. W. Pan, T. I. Hesla and D. D. Joseph, A fictitious domain approach to the direct numerical simulation of incompressible viscous flow past moving rigid bodies: application to particulate flow, Journal of Computational Physics, vol 169.2, 363-426, (2001).

[2] E. Lauga and T. R. Powers, The hydrodynamics of swimming microorganisms, Reports on Progress in Physics, vol 72.9, 096601, (2009).

[3] M. J. Lighthill, On the squirming motion of nearly spherical deformable bodies through liquids at very small Reynolds numbers, Communications on Pure and Applied Mathematics, Wiley Online Library, 109-118, (1952).

[4] A. Najafi and R. Golestanian, Simple swimmer at low Reynolds number: Three linked spheres, Physical Review E, vol 69.6, 062901, (2004).

[5] S. Paz Sánchez and G. C. Buscaglia, Simulating squirmers with volumetric solvers, arXiv preprint arXiv:1903.07753, (2019).

[6] D. Saintillan, E. Darve, and E. S. G. Shaqfeh, A smooth particle-mesh Ewald algorithm for Stokes suspension simulations: The sedimentation of fibers, Physics of Fluids, vol 17.3, 033301, (2005).

[7] A. C. H. Tsang, P. W. Tong, S. Nallan, and O. S. Pak, Self-learning how to swim at low Reynolds number, arXiv preprint arXiv:1808.07639, (2018).

[8] S. Verma, G. Novati, and P. Koumoutsakos, Efficient collective swimming by harnessing vortices through deep reinforcement learning, Proceedings of the National Academy of Sciences, vol 115.23, 5849-5854, (2018).